This is an author copy of the paper published in Electrochimica Acta 271 (2018) 203e210

Evolution of Pt and Ag nanoparticles composites with polyphenazines onto ITO electrodes during the oxidation of H_2O_2 with ascorbic acid

M. P. Rivas Romero, J. Gonzalez-Rodriguez [a], R. Rodríguez-Amaro, J.M. Rodríguez Mellado*

Departamento de Química Física y Termodinámica Aplicada. CEIA3, IUIQFN, Campus Universitario de Rabanales, edificio *Marie Curie*. Universidad de Córdoba. E-14014-Córdoba (Spain)

[a] School of Chemistry, University of Lincoln, Brayford Pool, Lincoln, LN6 7TS, United Kingdom

*Corresponding author (e-mail: jmrodriguez@uco.es)

Keywords: SEM-EDX; Raman Spectroscopy; electrocatalysis; polyphenazines; Pt and Ag nanoparticles.

Abstract

Six polyphenazine electrodes modified with platinum and silver nanoparticles deposited over conducting polymers have been prepared using electrochemical techniques. Phenazine monomers were electropolymerized on Indium tin oxide (ITO) and their morphology was explored by SEM-EDX and Raman spectroscopy. The main findings indicated that the polymers are not homogenously electrodeposited, having pores where metal nanoparticles can be nested, which can play an important role in the ionic exchange with the electrolyte. At longer deposition times, formation of clusters is observed with a loss of electrocatalytic activity and at shorter deposition times the growth step is not yet started and catalysis does not occur. Platinum nanoparticles with sizes of 10-60 nm are formed on the polymer agglomerates. Electrochemical measurements of H_2O_2 and H_2O_2-ascorbic acid were carried out as a model system and the electrodes have been characterized by SEM-EDX. The size of the nanoparticles and their aggregates decreased with respect to those of the original size. After an electrochemical cleaning, the sizes of aggregates were recovered which justify the reproducibility of the sensor. For Ag/Polymer/ITO, in all of cases, formation of dendrites plus silver nanoparticles was observed by SEM-EDX.

1. Introduction

Antioxidants play a relevant role in disease prevention and nutrition [1], in many cases by reacting with radicals generated in living organisms such as $HO^{\bullet}$, $HO_2^{\bullet}$ or $O_2^{\bullet -}$, called *reactive oxygen species* (ROS). These species are implied in oxidative stress [2] participating in the damage to proteins, DNA and lipids [3] and in chronic diseases [4]. Secondary antioxidants prevent the activation of carcinogens by interrupting the free radical propagation. The antioxidant capacity, related to the ability to capture ROS [5], is traditionally measured by using radicals such as $ABTS^{+\bullet}$ [6], $DPPH^{\bullet}$ [7] and through electrochemical methods, such as polarographic measurements on mercury electrodes [8, 9]. Very recently mercury has been restricted by health authorities and radicals measurements are performed far from physiological conditions. In a previous work, electrodes modified with conducting polymers and electrodeposited platinum nanoparticles were built [10]. The electrode made with poly-neutral red (PNR) was stable (for more than 5 months), reproducible and able to assess the scavenging ability of ascorbic acid. Cyclic Vis-NIR spectroelectrogravimetry and *ac*-electrogravimetry [11] helped to elucidate that radical cations localized in the inter-monomer bonds of the polymer were stabilized by platinum nanoparticles and, in the catalysed reduction of H_2O_2, the polymer acted as a proton reservoir. This electrode was used to assess the antioxidant activity of active principles present in foods, which were compared to those measurements obtained by the spectrophotometric DPPH radical scavenging method and the CUPRAC assay [12]. The measurement time and easiness were improved when compared to these standard methods achieving comparable sensitivity.

Polyphenazines, in the absence of nanoparticles, have been widely used [13, 14], especially in the construction of biosensors for hydrogen peroxide [15], to develop redox mediators [16, 17] and to study the electrocatalysis in the NADH oxidation [18, 19].

Glassy carbon electrodes modified with polyphenazine conducting polymers and Pt or Ag nanoparticles were prepared. These electrodes were used to study the interaction between H_2O_2 and antioxidants, in trolox equivalents, which was similar for all electrodes studied, and agreed with previously reported data using other contrasted techniques [20]. Recently, sensors for H_2O_2 have been designed using a nanocomposite of cobalt(III) complex and MWCNTs [21] or using cerium nanoparticles, which have been demonstrated to neutralize free radicals [22].

The aim of this paper is to study the evolution of composites of Pt and Ag nanoparticles with polyphenazines during the oxidation of H_2O_2 in the absence and in the presence of antioxidants, such as ascorbic acid, to justify the performance of these electrodes for the determination of antioxidant capacity. To reach this goal, a superficial characterization of the layers of conducting polymers covered with metal nanoparticles has been made to establish the way in which these particles are distributed and whether this morphology is related to the reproducibility and durability of the electrodes.

The structures of the monomers used to synthetize the conducting polymers are shown in Figure 1 and metals were platinum and silver.

-- Figure 1 --

2. Experimental

The monomers used were Neutral Red > 90% from Amresco, Safranine O > 90%, Phenosafranine 80%, Hexachloroplatinic acid 99.5%, Silver Nitrate ≥ 99.8%, Ascorbic Acid 99%, all from Sigma-Aldrich, and the rest of reactants from Merck. All reactants were analytical grade reagents and were used without further purification.

The supporting electrolyte used was 0.1 M PBS buffer at pH 7.0. The solutions were prepared using ultrapure type I (resistivity 18.2 MΩ.cm at 298 K) obtained from a Millipore water system. Stock solutions were stored in the dark at 277 K to avoid decomposition and H_2O_2 and antioxidant solutions were freshly prepared before each experiment.

Electrochemical measurements were made with an Autolab PGSTAT302N potentiostat and the NOVA 1.9 software package. A three-electrode cell equipped with a Pt wire counter electrode, a BAS MF-2079 Ag/AgCl 3 M KCl reference electrode was used. Indium tin oxide (ITO) (10x15 mm) was used as working electrode for electrochemical measurements and consequently, as substrate for characterization.

All tests were performed at 298 K. Surface characterization studies were carried out by means of scanning electron microscopy (SEM) and Raman spectroscopy. Regarding SEM, two instruments were employed: An FEI Inspect SEM attached to an INCA x-act EDX detector from Oxford Instruments (Abingdon, Oxfordshire, UK) using INCA Software operated at 15.0 kV and an emission current of 10.5 μA, at the University of Lincoln, and a JOEL JSM 7800F, Field Emission Scanning Electron Microscope with an acceleration voltage 5.0 kV and an emission current of 61.5 μA, at the University of Córdoba. Raman Spectroscopy measurements were performed with a HORIBA Jobin Yvon LabRaman spectrometer with holographic grating 1800 gr·mm^{-1}. Excitation line was provided by argon laser at 532 nm. Laser beam was focused through a Japan LMPlanFL N 50x/0.50 objective.

After an electrochemical cleaning, consisting in successive cyclic sweeps from 0.6V to -0.7V for 12 cycles on buffer electrolyte, electropolymerization was carried out. In the case of the poly-neutral red (PNR) deposition, 10 mg of neutral red were added to 40mL of 0.5 M H_2SO_4. The

electropolymerization potential range was from 1.3V to –0.5V and the scan rate was set at 50 mV s^{-1} for 10 cycles [10].

Regarding poly-safranine (PS) and poly-phenosafranine (PPs), 10 mg of monomer were added to 40mL of 0.1 M PBS solution at pH7, and the polymerization was performed by cycling in the potential range 1.2V to –0.8V and a scan rate of 50 mV s^{-1} for 15 cycles. All of solutions were deoxygenated by nitrogen pumping for 10 minutes [20].

Metal nanoparticles (MNPs), platinum and silver, were deposited by constant potential at -0.2V. A platinum solution made of $5 \cdot 10^{-3}$ M hexachloroplatinic acid solution in 0.5 M H_2SO_4 was used while the bulk solution for silver was made of $1 \cdot 10^{-3}$ M silver nitrate solution in 0.5 M H_2SO_4 [20]. Later, a new electrochemical cleaning was done by cyclic voltammetry in a 0.1 M PBS solution (–0.4V to 0.7V, at 100 mV s^{-1}, 2 cycles in most cases).

Once the electrodes were produced their surfaces were characterized by SEM and Raman. Subsequently, electrochemical measurements were carried out in the presence of hydrogen peroxide and hydrogen peroxide plus ascorbic acid and finally characterized again using SEM and Raman.

3. Results and discussion

3.1. Electrodeposition of Platinum Nanoparticles on the polymer layers

Prior to platinum deposition on the ITO electrodes, the surface has to be modified with polyphenazines. Polymerization of polyphenazines on ITO was carried out by cyclic voltammetry following the electropolymerization conditions previously reported in the literature [10, 20] and

summarized in the previous section. Figure 2 shows the voltammograms recorded in the course of the electropolymerization.

-- Figure 2 --

In all cases, two reversible redox systems appeared in the first cycle of the electropolymerization. A reversible redox system appears at negative potentials, corresponding to the monomer and accompanied by oxidation peaks at highly positive potentials, with intensity changing in successive scans to reach a constant value. The signals corresponding to the monomer decrease and this redox system eventually disappear, meaning that the monomer is consumed, and the polymer is growing up. This behaviour is similar to those observed for other electrodes in the literature [23, 24]. For PPs and PS, the presence of the phenyl radical with free rotation causes a steric hindrance in the growth of the polymer and the layers of polymer reaches a limit. In the case of PS, after 20-25 cycles the polymer layer has a constant thickness probably due to the additional hindrance provided by the methyl groups of the molecule [20].

Figure 3 shows the SEM image of PNR after the electropolymerization on the electrode. As it can be seen, the polymer is not electrodeposited in a homogenous way and its surface distribution is granular. The deposit thickness is not constant due to existence of “mountain-valley” features and the electrode surface presents gaps not covered by the polymer. However, inside the polymer granules some pores may be formed and Pt nanoparticles could be nested. These pores are interesting because of their important role concerning ionic exchange with the electrolyte [11]. The average diameter of the polymer granules was observed to be 799 nm.

-- Figure 3 --

Mapped Raman spectra confirmed that the distribution of polymer is not homogenous. The bands corresponding to the different vibration modes (mainly deformation and stretching) for the phenyl ligand, the quinone structure and the phenazine ring (1000 - 1750cm^{-1} region) were observed. It is important to highlight those corresponding to the C-N tension of the secondary aromatic amine (1356 cm^{-1}), which are not observed for the monomer [25].

Figure 4 shows the SEM images of PNR after the electrochemical deposition of Pt nanoparticles at different deposition times.

-- Figure 4 --

In these images, it can be observed that the polymer is covered by Pt nanoparticles forming aggregates. The size of the nanoparticles aggregates gradually increases with longer deposition times. In all cases, nanoparticles average size was obtained by using a Gauss distribution, as seen in figure S1 in the supplementary material.

For longer electrodeposition times, the peak intensity for the voltammograms corresponding to the hydrogen peroxide reduction decreased, and was displaced somewhat to more negative potentials. This implies a loss of the electrocatalytic activity of hydrogen peroxide on this electrode. The formation of big clusters also observed must be related with this phenomenon. For shorter times, catalysis does not happen due to absence of the growth step. Moreover, it can be appreciated that the agglomerates on the polymer are integrated by PtNPs with a size between 10-60 nm (at 60 s). The morphology, size and occupied sites of platinum on agglomerates of the polymer confers the electrocatalytic properties to the sensor.

The nanocomposite Pt/PNR/ITO was also characterized by Raman. Figure 5 shows the spectra of PNR and Pt/PNR/ITO. The spectrum corresponding to PNR shows bands appearing in the range 1000-1750 cm^{-1} corresponding to vibrations, deformations and tensions from both the quinone

structure and the phenazine ring. The more important bands appear at 1576 cm^{-1}, which correspond to the tension of quinone ring. At 1510 cm^{-1} and 1356 cm^{-1} the stretching of penta-substituted rings and the tension of the C-N bond of the secondary amine can be respectively observed, which is in accord with the polymer formation. At 1153 cm^{-1} the C-N-C vibration of the tertiary amino group can be also observed [25]. The bands appearing in this range are attenuated by the presence of platinum as the wavelength range 350-410 cm^{-1} corresponding to Pt-Ox or Pt-OH vibrations [26, 27]. The presence of Platinum is confirmed by EDX measurements (see figure S2 in supplementary material).

-- Figure 5 --

The SEM images of poly-safranine and poly-phenosafranine supported on ITO also show agglomerates of polymer, containing the "mountain and valley" features as in the case of PNR. When platinum is deposited at –0.2V and different deposition times, these polymeric agglomerates are covered by platinum nanoparticles, which are also located in the polymer pores. Moreover, Pt aggregates do not coat completely the polymer, as it happened for the PNR system and shown in figure 6. Both morphologies have been also contrasted by Raman spectroscopy. Figure S3 in supplementary material shows the spectra of the three polyphenazines, in order to clarify the origin of the bands [25, 28]. In addition, figure S4 in supplementary material shows the spectra of Pt/PS/ITO and Pt/PPs/ITO before and after the deposition of Pt nanoparticles. The interpretation of these graphs is the same as for Pt/PNR/ITO.

--Figure 6--

3.2. Electrodeposition of Silver Nanoparticles on the polymer layers

With the aim to explore the catalytic behavior of other metals and also to bring down the cost of the potential sensors, the use of silver nanoparticles was tested. These were deposited using a

$1 \cdot 10^{-3}$ M $AgNO_3$ solution in 0.5 M H_2SO_4 at –0.2V, different deposition times [20] and on top of a previously formed polyphenazine layer obtained by using electropolymerization performed by cyclic voltammetry.

For Ag/PNR/ITO, the formation of dendrites plus silver nanoparticles was also observed by SEM at any deposition time. These dendrites and nanoparticles cover the agglomerates of polymers and are also nested within them, as confirmed by SEM-EDX and Raman spectroscopy (see figure 5). As it can be seen in the Raman spectrum, the region between 215-240 cm^{-1} shows a typical band from Ag-Ox vibrations as contrasted in the literature [29]. The main bands corresponding to the polymer vary in intensity due to the silver presence, as it happened in the Pt/PNR/ITO system. Raman of PS and PPS doped by Ag nanoparticles are very similar to those shown in Figure S4 in supplementary material. EDX confirms the presence of silver (Figures S2 and S5 in supplementary material).

In the SEM images shown in figure 7, it can be observed that the electrochemical surface coverage increases continuously as the deposition time increases. However, at longer times most of the deposited silver layers are brittle and de-attach from the electrode because the polymer is not able to hold them all. Moreover, both Raman and SEM show that silver nanoparticles and silver dendrites do not coat the polymer completely. To evaluate the progression in the formation of the silver aggregates, the size of these polymer aggregates was analysed, as shown in figure 7.

-- Figure 7 –

As the deposition time increases, the size of silver dendrites also increases, but at shorter times the silver nanoparticles formation prevails.

3.3. Effect of the electrooxidation of hydrogen peroxide on the morphology of Pt-nanoparticles

Electrochemical measurements of the reduction of H_2O_2 in the absence and in the presence of ascorbic acid were carried out. Both electrochemical experiments are recorded in figure 8. In the first one, the reduction signal is increasing due to the presence of free radicals from hydrogen peroxide in the media, however, in the second one, the reduction signal is decreasing because of the presence of antioxidant, ascorbic acid, which acts as reducing agent avoiding the oxidation of free radicals.

-- Figure 8 –

The size of platinum nanoparticles decreased in the presence of hydrogen peroxide, as can be seen in figure 9. These decreased again when the experiment was made in the presence of ascorbic acid, as it is shown if figure S6 in supplementary material. However, when an electrochemical cleaning was carried out the size of the platinum nanoparticles was recovered, justifying the reproducibility of the sensor. The regeneration of the nanoparticles morphology also occurs after the electrochemical cleaning is carried out for electrodes used for the experiments in the presence of ascorbic acid. This is also the case for the electrodes made with polysafranine and polyphenosafranine and platinum nanoparticles. The catalysis of hydrogen peroxide is worse for the Pt/PNR/ITO system, as it can be seen in figures S7-S9 in supplementary material, probably due to the presence of the phenyl ligand which could affect to the nesting of nanoparticles. The results obtained with silver modified electrodes showed that the changes experimented by the dendrites is irreversible, this accounting for the less reproducibility of these electrodes.

-- Figure 9 –

4. Conclusions

Six polyphenazine electrodes modified with metal nanoparticles deposited over conducting polymers have been prepared using electrochemical techniques. Phenazine monomers were electropolymerized on Indium tin oxide (ITO) and their morphology was explored by SEM-EDX and Raman spectroscopy. Results showed that the polymers are not homogenously electrodeposited, having pores where metal nanoparticles can be nested, which can play an important role in the ionic exchange with the electrolyte. At longer times, formation of clusters is observed with a loss of electrocatalytic activity, and at shorter times the growth step is not yet started, and catalysis does not occur. Platinum nanoparticles with sizes of 10-60 nm are formed on the polymer agglomerates. Electrochemical measurements of H_2O_2 and H_2O_2-ascorbic acid were carried out and the electrodes have been characterized by SEM-EDX. The size of the nanoparticles and their aggregates decreased respect to the original size. After an electrochemical cleaning, the sizes of aggregates were recovered which justify the reproducibility of the sensor. For Ag/Polymer/ITO, in all of cases formation of dendrites plus silver nanoparticles was observed by SEM-EDX.

5. References

1. J. M. C. Gutteridge, B. Halliwell, Free radicals and antioxidants in the year 2000: a historical look to the future, Ann. N. Y. Acad. Sci. 899 (2000) 136.

2. M.L. Circu, M.L. and T.Y. Aw, Reactive oxygen species, cellular redox systems, and apoptosis, Free Radic. Biol. Med.48 (2010) 749.

3. C. Bailly, H. Ei-Maarouf-Bouteau, and F. Corbineau, From intracellular signalling networks to cell death: the dual role of reactive oxygen species in seed physiology, Comptes Rendues Biol. 331 (2008) 806.

4. A. Barzilai and K. Yamamoto, DNA damage response to oxidative stress, DNA Repair. 3 (2004) 1109.

5. J. F. Arteaga, M. Ruiz Montoya, A. Palma, G. Alonso Garrido, S. Pintado, J. M. Rodríguez Mellado, Simple Electrochemical Method for the Fast Determination of Antioxidant Capacity of Active Principles: Comparison with DPPH Assay, Molecules, 17 (2012) 5126.

6. Bendini, A.; Toschi, T.G.; Lercher, G. Determination of the antioxidant activity of vegetable extracts by Oxidative Stability Instrument (OSI). Ind. Aliment. 403 (2001) 525.

7. Kahkonen, M.P.; Hopia, A.; Vuorela, H.; Rahua, J.P.; Pihlaja, K.; Kujala, T.; Heinonen, M. Antioxidant activity of plant extracts containing phenolic compounds. J. Agric. Food Chem. 47 (1999) 3954.

8. D. Ž. Sužnjević, F. T. Pastor, S. Ž. Gorjanović, Polarogaphic study of hydrogen anodic current and its application to antioxidant activity determination, Talanta, 85 (2011) 1398.

9. A. Palma, M. Ruiz Montoya, J. F. Arteaga and J. M. Rodríguez Mellado, Determination of antioxidant activity of spices and their active principles by differential pulse voltammetry J. Agric. Food Chem. 62 (2014) 582.

10. P. Rivas, J.M. Rodríguez Mellado, Seeking a reliable electrode for the monitoring of the hydrogen peroxide reduction in the presence of antioxidants, Electrochim. Acta 171 (2015) 150.

11. J. Agrisuelas, J.J. García-Jareño, P. Rivas, J.M. Rodríguez Mellado, F. Vicente, Electrochemistry and electrocatalysis of a Pt@poly(neutral red) hybrid nanocomposite, Electrochim. Acta 171 (2015) 165.

12. M. P. Rivas Romero, R. Estevez Brito,A. Palma, M. Ruiz Montoya, J.M. Rodríguez Mellado, and Rafael Rodríguez -Amaro, J. Electrochem. Soc. 164 (2017) B97.

13. R. Pauliukaite, M. E. Ghica, M. M. Barsan, C. M. A. Brett, Phenazines and polyphenazines in electrochemical sensors and biosensors, Anal. Lett. 43 (2010) 1588.

14. M. M. Barsan, M. E. Ghica, C. M. A. Brett, Electrochemical sensors and biosensors based on redox polymer/carbon nanotube modified electrodes: A review, Anal. Chim. Acta 881 (2015) 1.

15. A. Attar, M.E. Ghica, A. Amine, C.M.A. Brett, Poly(neutral red) based hydrogen peroxide biosensor for chromium determination by inhibition measurements, J. Hazard. Mater. 279 (2014) 348.

16. A.-M. Chiorcea-Paquim, R. Pauliukaite, C.M.A. Brett, A.M. Oliveira-Brett, AFM nanometer surface morphological study of in situ electropolymerized neutral red redox mediator oxysilane sol-gel encapsulated glucose oxidase electrochemical biosensors, Biosens. Bioelectron. 24 (2008) 297.

17. A.A. Karyakin, E.E. Karyakina, W. Schuhmann, H.-L. Schmidt, Electropolymerized Azines: Part II. In a Search of the Best Electrocatalyst of NADH Oxidation, Electroanalysis. 11 (1999) 553.

18. A.A. Karyakin, O.A. Bobrova, E.E. Karyakina, Electroreduction of NAD^+ to enzymatically active NADH at poly(neutral red) modified electrodes, J. Electroanal. Chem. 399 (1995) 179.

19. R. Pauliukaite, C.M.A. Brett, Poly(neutral red): Electrosynthesis, characterization, and application as a redox mediator, Electroanalysis. 20 (2008) 1275.

20. M.P. Rivas Romero, J.M. Luque Centeno, R. Estévez Brito, R. Rodríguez-Amaro, J.M. Rodríguez Mellado, Application of polyphenazine films doped with metal nanoparticles for the measurements of antioxidant capacity, Journal of Electroanalytical Chemistry 789 (2017) 24

21. C. M.Parnell, F. Watanabe, U. B.Nasini, B. C. Berry, T. Mitchell, A. U. Shaikh, A. Ghosh, Electrochemical sensing of hydrogen peroxide using a cobalt(III) complex supported on carbonaceous nanomaterials, Scientific Reports 7 (2017) Article number: 1324.

22. C. J. Neal, A. Gupta, S. Barkam, S. Saraf, S. Das, H. Cho, S. Seal, Electrochemical sensing of hydrogen peroxide using a cobalt(III) complex supported on carbonaceous nanomaterials. J. Electroanal. Chem. 740 (2015) 37.

23. D. Benito, C. Gabrielli, J.J. García-Jareño, M. Keddam, H. Perrot, F. Vicente, Study by EQCM on the voltammetric electrogeneration of poly(neutral red). The effect of the pH and the nature of cations and anions on the electrochemistry of the films, Electrochim. Acta, 48 (2003) 4039.

24. T. Komura, M. Ishihara, T. Yamaguchi, K. Takahashi, Charge-transporting properties of electropolymerized phenosafranin in aqueous media. J. Electroanal. Chem. 493 (2000) 84

25. G. Broncová, T. V. Shishkanova, P. Matějka, R. Volf, V. Král, Citrate selectivity of poly(nuetral red) electropolymerized films, Anal. Chim. Acta 511 (2004) 197.

26. R. Jiménez-Pérez, J.M. Sevilla, T. Pineda, M. Blázquez, J. Gonzalez-Rodriguez, Comparative study of ϒ-hidroxybutiric acid (GHB) and other derivative compounds by spectroelectrochemistry raman (SERS) on platinum surface, Electrochim. Acta. 193 (2016) 154.

27. R. Jiménez-Pérez, J.M. Sevilla, T. Pineda, M. Blázquez, J. Gonzalez-Rodriguez, Study of the electro-oxidation of a recreational drug GHB (gamma hydroxybutyric acid) on a platinum catalyst-type electrode through chronamperometry and spectro-electrochemistry, J. Electroanal. Chem. 766 (2016) 141.

28. G. Ćirić-Marjanović, N.V. Blinova, M. Trchová, J. Stejskaal, The chemical oxidative polymerization of safranines, J. Phys. Chem. B. 111 (2007) 2188.

29. G. Naja, P. Bouvrette, S. Hrapovic, J.H.T. Luong, Raman-based detection of bacteria using silver nanoparticles conjugated with antibodies, Analyst 132 (2007) 679.

Figure headings

Scheme 1. Chemical structures of the monomers.

Figure 2. Electropolymerization of polyphenazines on ITO electrodes. Details on the experimental section. Red: first scans. Arrows indicate the initial potential and scan direction.

Figure 3. Left, top and down: SEM images of PNR/ITO. Acceleration voltage of 15kV, 5.0kV, magnification of x1.5k, x16k and working distance of 15 mm, 10 mm. Right: Histogram for polymer particles sizes. The red line corresponds to a Gaussian distribution fit.

Figure 4. SEM images for Pt/PNR/ITO at different platinum deposition times. Acceleration voltage of 15Kv, magnification of x2k and working distance of 15 mm, for most of the cases.

Figure 5. Top: Raman spectra of Pt/PNR/ITO and Raman microscope photography of Pt/PNR/ITO at 60s platinum deposition time. Down: Raman spectra of Ag/PNR/ITO at 60s silver deposition time.

Figure 6. SEM images. Acceleration voltage 20kV, magnification x2100 and working distance 15 mm. Top: PS. Down: PPs. Left: ITO covered by the polymers. Center: Pt deposition (60 s). Right: Ag deposition (60 s).

Figure 7. SEM images of Ag/PNR/ITO at different silver deposition times. Acceleration voltage of 20kV, magnification of x2100 and working distance of 15 mm.

Figure 8. Differential pulse voltammetry of H_2O_2 on Pt/PNR/ITO in PBS at pH 7.0 scan rate 0.1 $V \cdot s^{-1}$. Top: using different H_2O_2 concentrations. Down: using $2.5 \cdot 10^{-3}$ M H_2O_2 concentration and different ascorbic acid concentrations. Arrows indicate the initial potential and scan direction.

Figure 9. SEM images obtained after recording the oxidation signal of $2.5 \cdot 10^{-3}$ M H_2O_2 in the absence (A) and in presence of $1.25 \cdot 10^{-3}$ M ascorbic acid, AA (B) on the electrodes covered by platinum during 60 s. Up: Pt/PNR/ITO. Center: Pt/PS/ITO. Down: Pt/PPs/ITO.

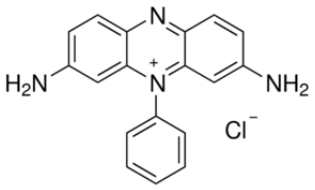

Phenosafranine (Ps)

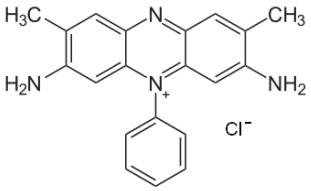

Safranine O (S)

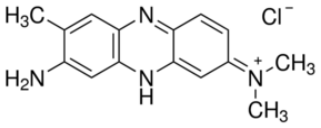

Neutral Red (NR)

Figure 1

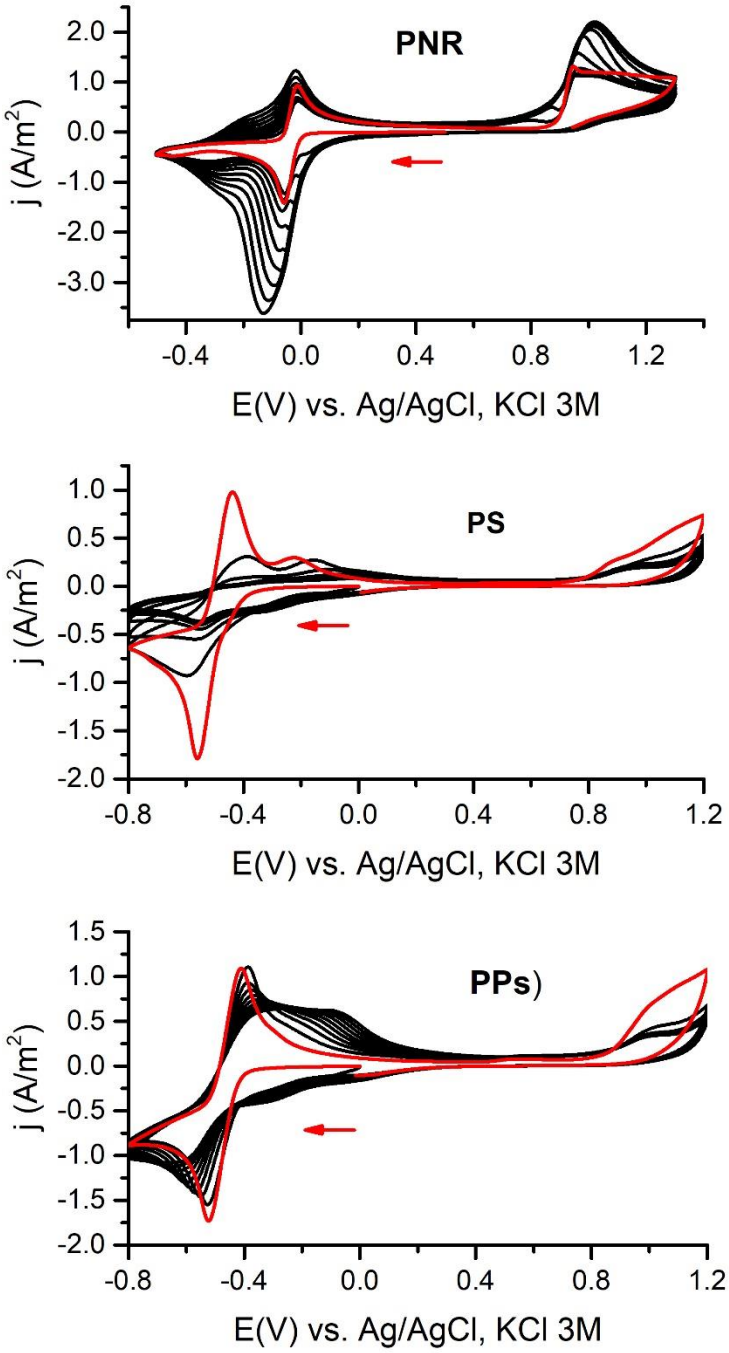
PNR
j (A/m²)
E(V) vs. Ag/AgCl, KCl 3M
PS
j (A/m²)
E(V) vs. Ag/AgCl, KCl 3M
PPs)
j (A/m²)
E(V) vs. Ag/AgCl, KCl 3M

Figure 2

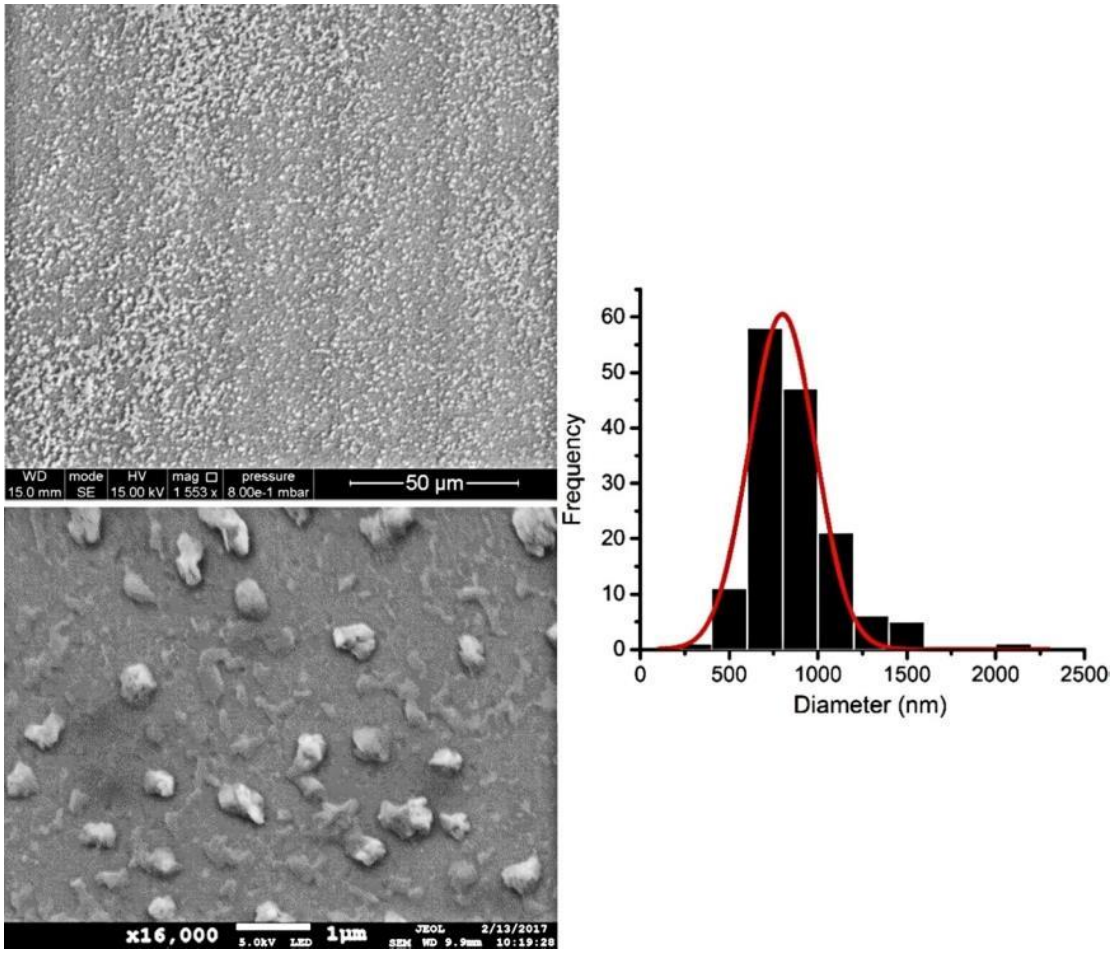
WD
15.0 mm
mode
SE
HV
15.00 kV
mag
1 553 x
pressure
8.00e-1 mbar
50 µm
x16,000
5.0kV LED
1µm
JEOL
SEM WD 9.9mm
2/13/2017
10:19:28
Frequency
Diameter (nm)
0
10
20
30
40
50
60
0
500
1000
1500
2000
2500

Figure 3

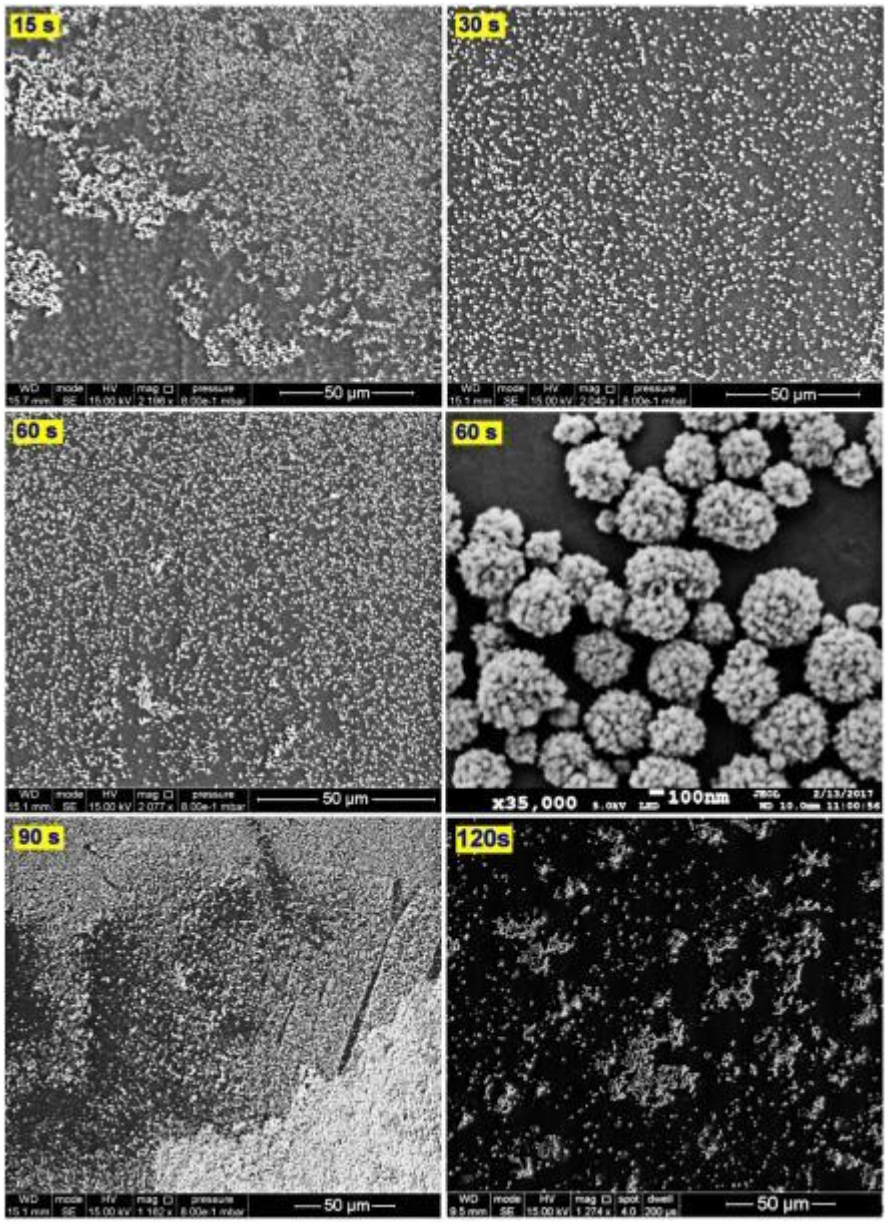
15 s
50 µm
30 s
50 µm
60 s
50 µm
60 s
x35,000
100nm
90 s
50 µm
120s
50 µm

Figure 4

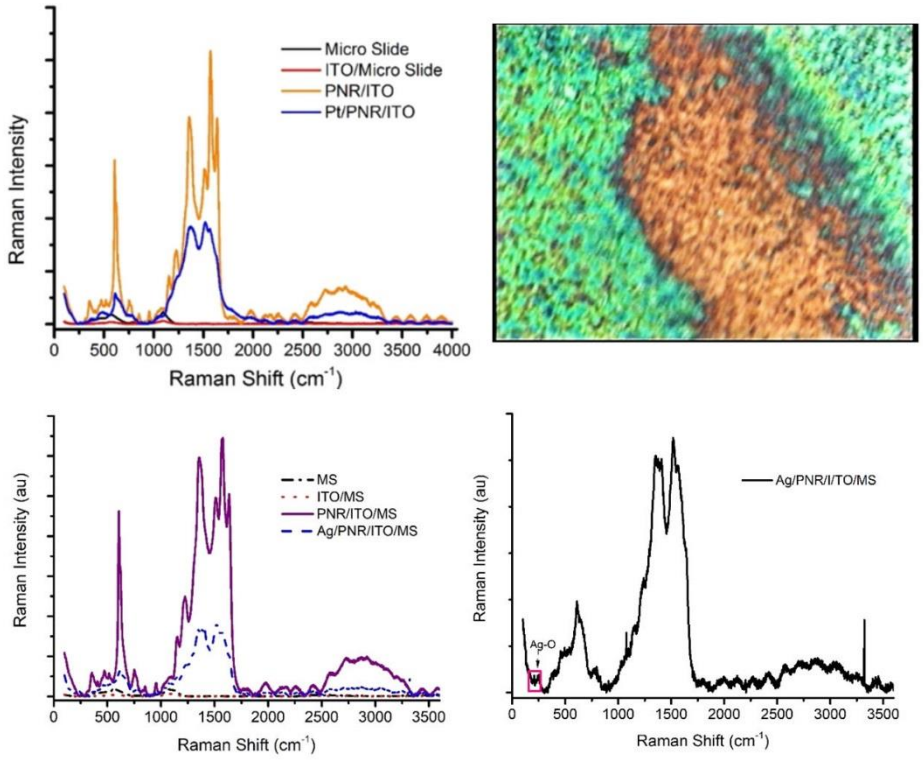

Figure 5

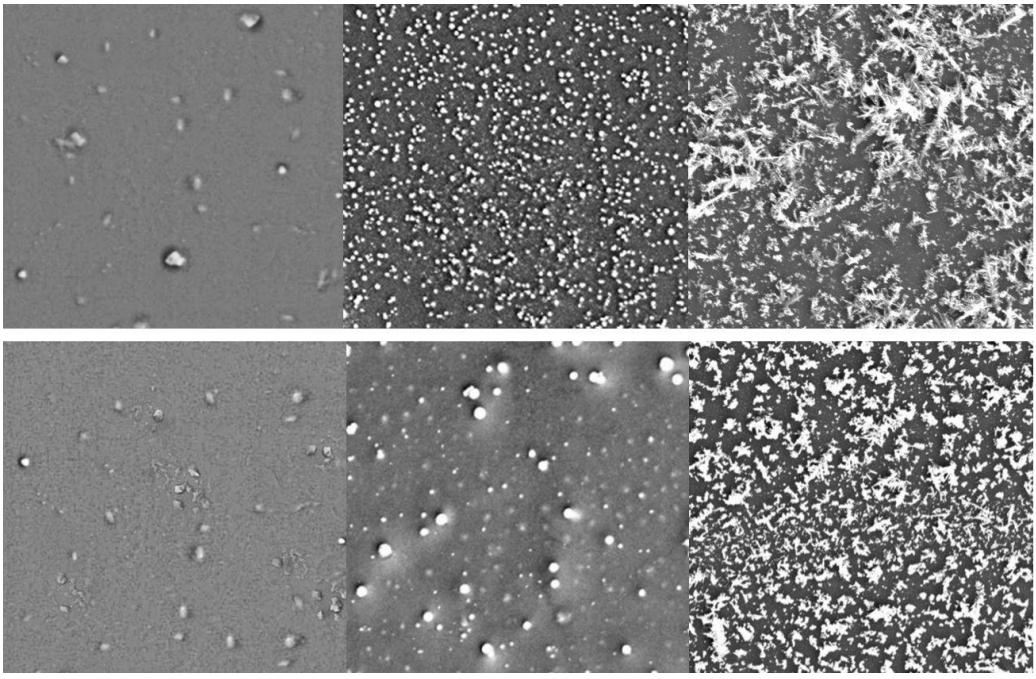

Figure 6

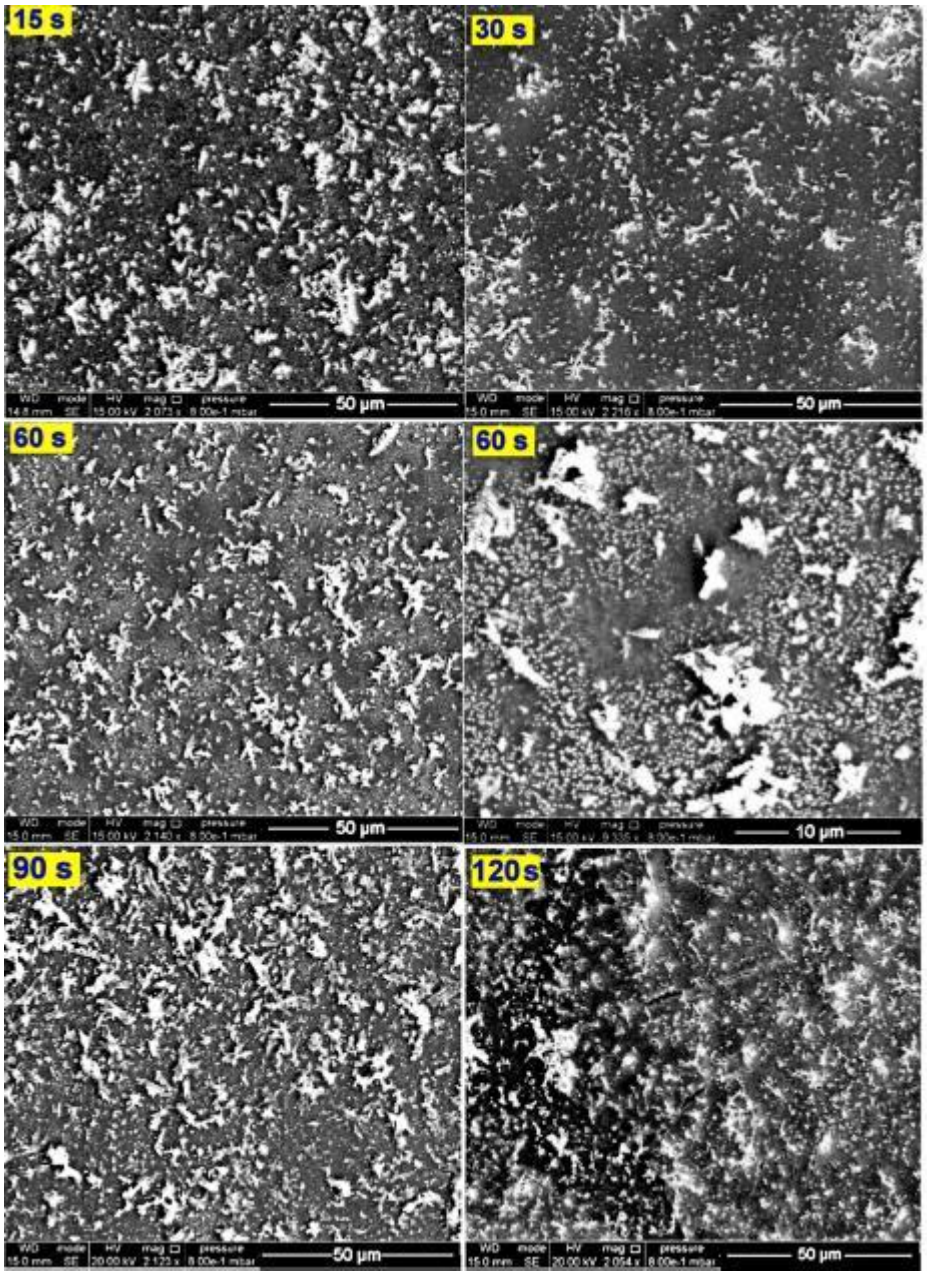

Figure 7

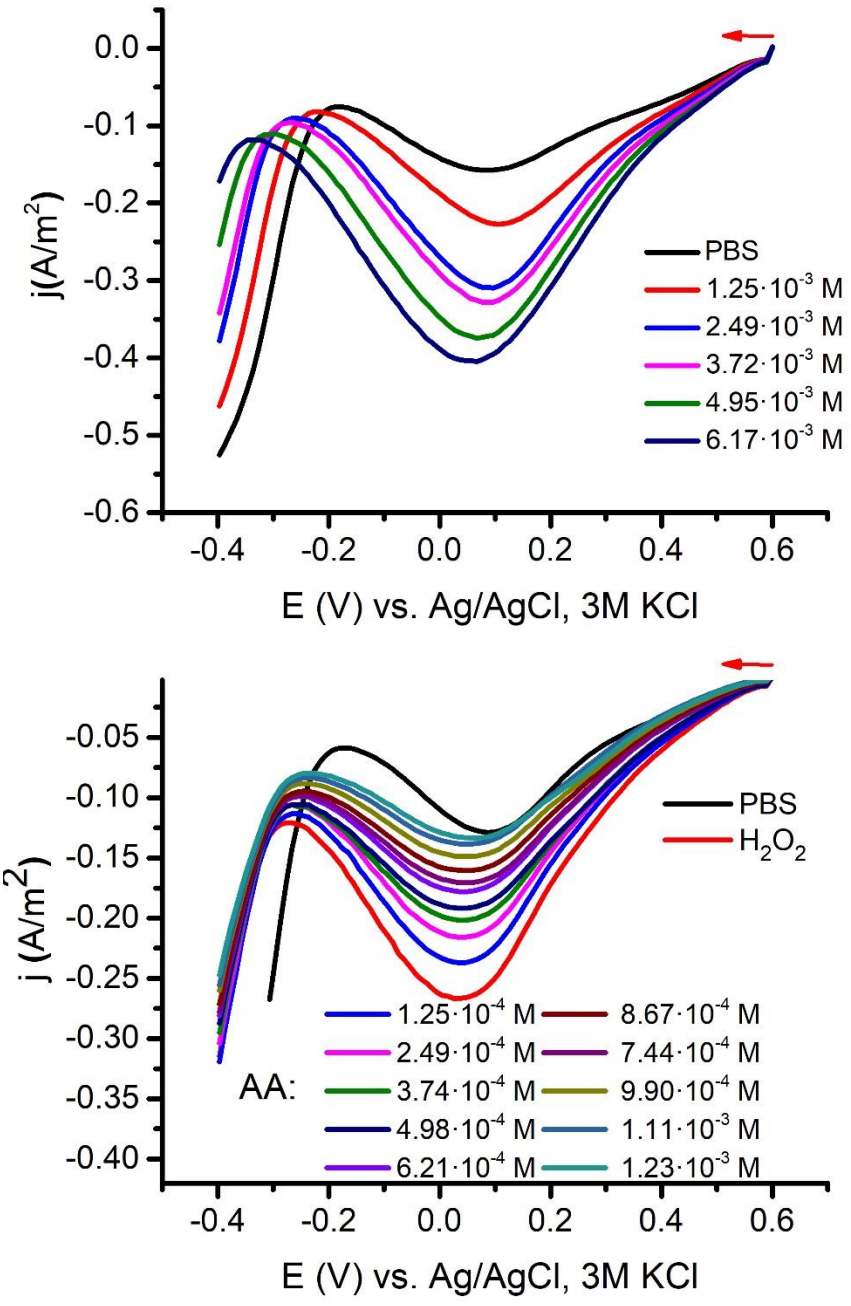
0.0
-0.1
-0.2
-0.3
-0.4
-0.5
-0.6
j(A/m²)
-0.4
-0.2
0.0
0.2
0.4
0.6
E (V) vs. Ag/AgCl, 3M KCl
PBS
1.25·10⁻³ M
2.49·10⁻³ M
3.72·10⁻³ M
4.95·10⁻³ M
6.17·10⁻³ M
-0.05
-0.10
-0.15
-0.20
-0.25
-0.30
-0.35
-0.40
j (A/m²)
E (V) vs. Ag/AgCl, 3M KCl
PBS
H2O2
AA:
1.25·10⁻⁴ M
2.49·10⁻⁴ M
3.74·10⁻⁴ M
4.98·10⁻⁴ M
6.21·10⁻⁴ M
8.67·10⁻⁴ M
7.44·10⁻⁴ M
9.90·10⁻⁴ M
1.11·10⁻³ M
1.23·10⁻³ M

Figure 8

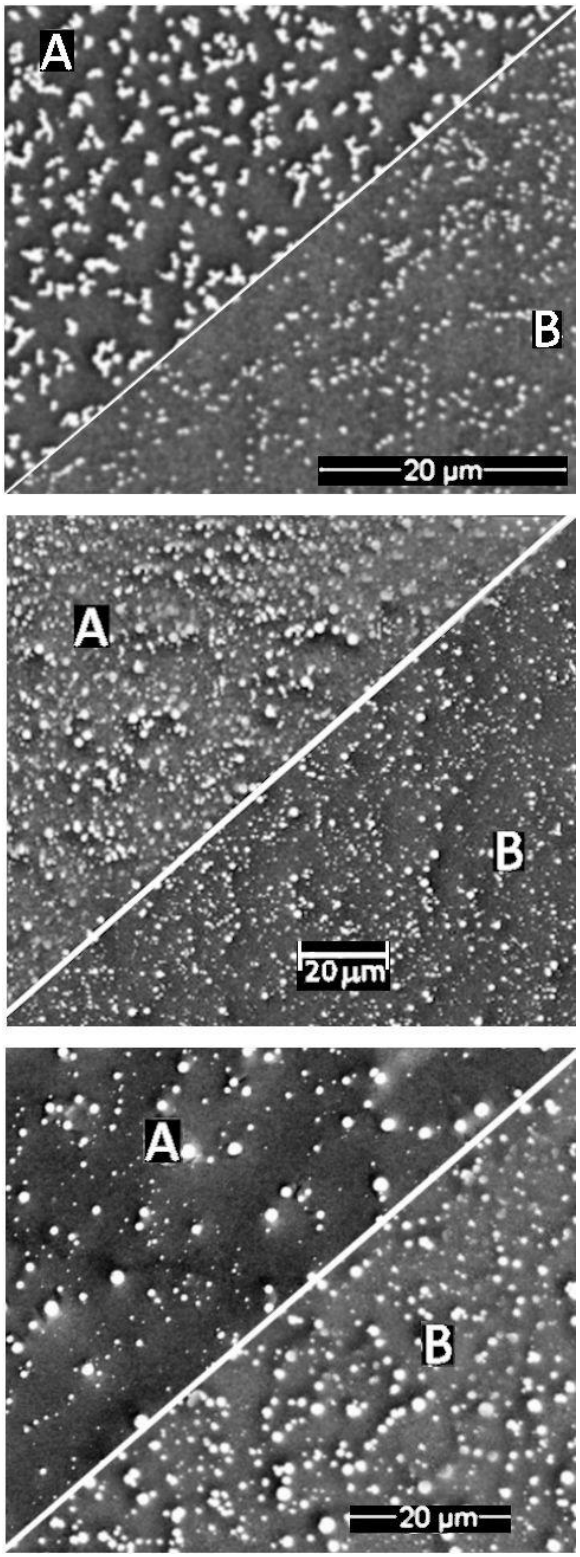

Figure 9